AGU PUBLICATIONS

JGR

Journal of Geophysical Research: Space Physics

RESEARCH ARTICLE
10.1002/2017JA024276

Key Points:
- Although two-equinox pattern in geomagnetic variation is seen in multiyear averages, only one fourth of individual years show this pattern
- One third of the years in 1966–2014 have a seasonal maximum at either solstice
- Seasonal variation of high-latitude geomagnetic activity follows solar wind speed in most years

Correspondence to:
E. I. Tanskanen,
eija.tanskanen@aalto.fi

Citation:
Tanskanen, E. I., Hynönen, R. & Mursula, K. (2017). Seasonal variation of high-latitude geomagnetic activity in individual years. *Journal of Geophysical Research: Space Physics*, *122*, 10,058–10,071. https://doi.org/10.1002/2017JA024276

Received 22 APR 2017
Accepted 23 SEP 2017
Accepted article online 29 SEP 2017
Published online 14 OCT 2017

Seasonal Variation of High-Latitude Geomagnetic Activity in Individual Years

E. I. Tanskanen[1], R. Hynönen[1], and K. Mursula[2]

[1]ReSoLVE Centre of Excellence, Aalto University, Espoo, Finland, [2]Space Climate Research Unit, ReSoLVE Centre of Excellence, Oulu University, Oulu, Finland

Abstract We study the seasonal variation of high-latitude geomagnetic activity in individual years in 1966–2014 (solar cycles 20–24) by identifying the most active and the second most active season based on westward electrojet indices *AL* (1966–2014) and *IL* (1995–2014). The annual maximum is found at either equinox in two thirds and at either solstice in one third of the years examined. The traditional two-equinox maximum pattern is found in roughly one fourth of the years. We found that the seasonal variation of high-latitude geomagnetic activity closely follows the solar wind speed. While the mechanisms leading to the two-equinox maxima pattern are in operation, the long-term change of solar wind speed tends to mask the effect of these mechanisms for individual years. Large cycle-to-cycle variation is found in the seasonal pattern: equinox maxima are more common during cycles 21 and 22 than in cycles 23 or 24. Exceptionally long winter dominance in high-latitude activity and solar wind speed is seen in the declining phase of cycle 23, after the appearance of the long-lasting low-latitude coronal hole.

1. Introduction

Geomagnetic activity has been monitored at a range of latitudes, including high (auroral and beyond) latitudes (Birkeland, 1908) for more than a century by ground-based magnetic measurements. Geomagnetic activity maximizes, on average, around the two equinoxes in spring and fall (Cliver, Kamide, & Ling, 2000; Clúa de Gonzales et al., 2001; Currie, 1966; Mursula, Tanskanen, & Love, 2011; Russell & McPherron, 1973; Sabine, 1856). This variation has been attributed to three main external effects: variation of the angle between the geocentric solar magnetospheric equatorial plane and the solar equatorial plane, also called the Russell-McPherron effect (Russell & McPherron, 1973), the equinoctial mechanism (Cliver et al., 2000; Lyatsky, Newell, & Hamza, 2001), and the change of the heliographic latitude of the Earth during the year, also called the axial effect (Cortie, 1912; McIntosh, 1959).

The two-equinox pattern of the seasonal variation of geomagnetic activity, which will be shown in section 3 in more detail, has typically been based on a superposed epoch (SPE) analysis, where the seasonal distributions of several years are combined to an average seasonal variation. In this paper we examine the seasonal variation in high-latitude geomagnetic activity in individual years in 1966–2014 using the *AL* and *IL* indices and compare that to the seasonal variation in solar wind speed, the main driver of high-latitude geomagnetic activity. We will study how often the two-equinox pattern is seen in individual years. Are two-equinox peaks seen consistently in individual years, or does the superposition of years with one equinox maximum give rise to the average two-equinox distribution? Conversely, how often does the annual maximum occur during either of the two solstices? We will also show that there are systematic but temporarily limited changes in the seasonal pattern and that there is a sequence of consecutive years when the seasonal maximum occurs during solstice rather than equinox.

We examine the seasonal variation of *high-latitude* geomagnetic activity because high-latitude geomagnetic activity better responds to the high-speed solar wind streams (HSSs) originated from large solar coronal holes than geomagnetic activity at low latitude to midlatitude, where coronal mass ejections (CMEs) have a relatively larger role (Finch et al., 2008; Holappa, Mursula, Asikainen, & Richardson, 2014). Moreover, most studies of the seasonal variation of geomagnetic activity are based on low-latitude to midlatitude observations and indices, and only relatively few studies (e.g., Cliver et al., 2000; Finch et al., 2008; McPherron, Hsu, & Chu, 2015; Mursula et al., 2011; Tanskanen et al., 2011) have examined the seasonal variation of geomagnetic activity at high latitudes.

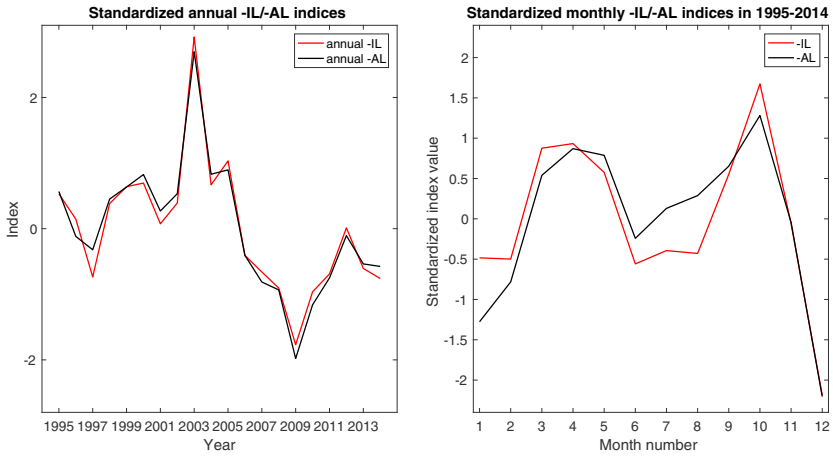

Figure 1. (left) Solar cycle evolution of high-latitude geomagnetic activity based on the $-IL$ and $-AL$ westward electrojet indices (1995–2014). (right) Superposed seasonal variation of the $-IL$ and $-AL$ indices for 1995 to 2014.

2. Data

We have used two geomagnetic activity indices, *AL* and *IL*, together with solar wind speed observations to examine the seasonal variation of high-latitude geomagnetic activity and its relationship to the solar wind speed at monthly time scales. Most geomagnetic activity indices use midlatitude observations, characterizing thereby mainly the midlatitude activity. The auroral electrojet indices *AE*/*AL*/*AU* aim to estimate geomagnetic activity at auroral latitudes (roughly 65°–75° of geomagnetic latitude), using observations at 12 magnetic stations roughly evenly located around the northern hemispheric auroral oval (Davis & Sugiura, 1966). We use here the westward electrojet *AL* index from the year 1966 onward in this analysis.

Dedicated meridional networks of magnetometers have been formed to better catch geomagnetic activity over a wide latitude range in a limited local time sector. International Monitor for Auroral Geomagnetic Effects (IMAGE) network (Syrjäsuo et al., 1998; Tanskanen, 2009) is one of these meridional networks, which started continuous operations in 1982. The *IL* index is based on data from 32 ground-based magnetic stations of the IMAGE network and calculated as another index of westward electrojet (Kallio et al., 2000) in a way analogous to the *AL* index. The *IL* index is now available for the analysis from 1995 to 2014. In this study we use also the *IL* index to study the pattern of seasonal variation of geomagnetic activity at high latitudes in individual years and to compare how accurately the solar wind speed modulates the high-latitude geomagnetic activity and reproduces the same seasonal pattern. We use monthly means of solar wind speed obtained from the hourly values of solar wind speed in the OMNI-2 database of the NASA National Space Science Data Center (NSSDC).

3. Seasonal Variation of *IL* and *AL* in 1995–2014

The seasonal variation of high-latitude geomagnetic activity is examined here by using the above mentioned westward electrojet indices *IL* and *AL*. The standardized, absolute values of the annually averaged *AL* and *IL* indices in 1995–2014 (time interval when *IL* is available) are shown in Figure 1 (left). Standardization was done by first removing the mean of the time series of absolute annual averages, and then dividing it by its standard deviation. Standardization was used in order to show the closely similar long-term evolution of the two indices despite their different absolute levels. (Note also that a westward current reduces the magnetic field on the ground; the more negative indices correspond to more disturbed times. We took the absolute value in order to have the largest disturbance to correspond to the highest value, which is more intuitive). The two indices show a very similar long-term evolution of high-latitude geomagnetic activity, with the largest annual activity in 2003 and the lowest in 2009.

Figure 1 (right) depicts the superposed seasonal variation for the two indices in 1995–2014 using the absolute values of the monthly means of the indices. We first calculated the monthly means for each month, then took their absolute values and then standardized them (for the same reasons as above). The superposed

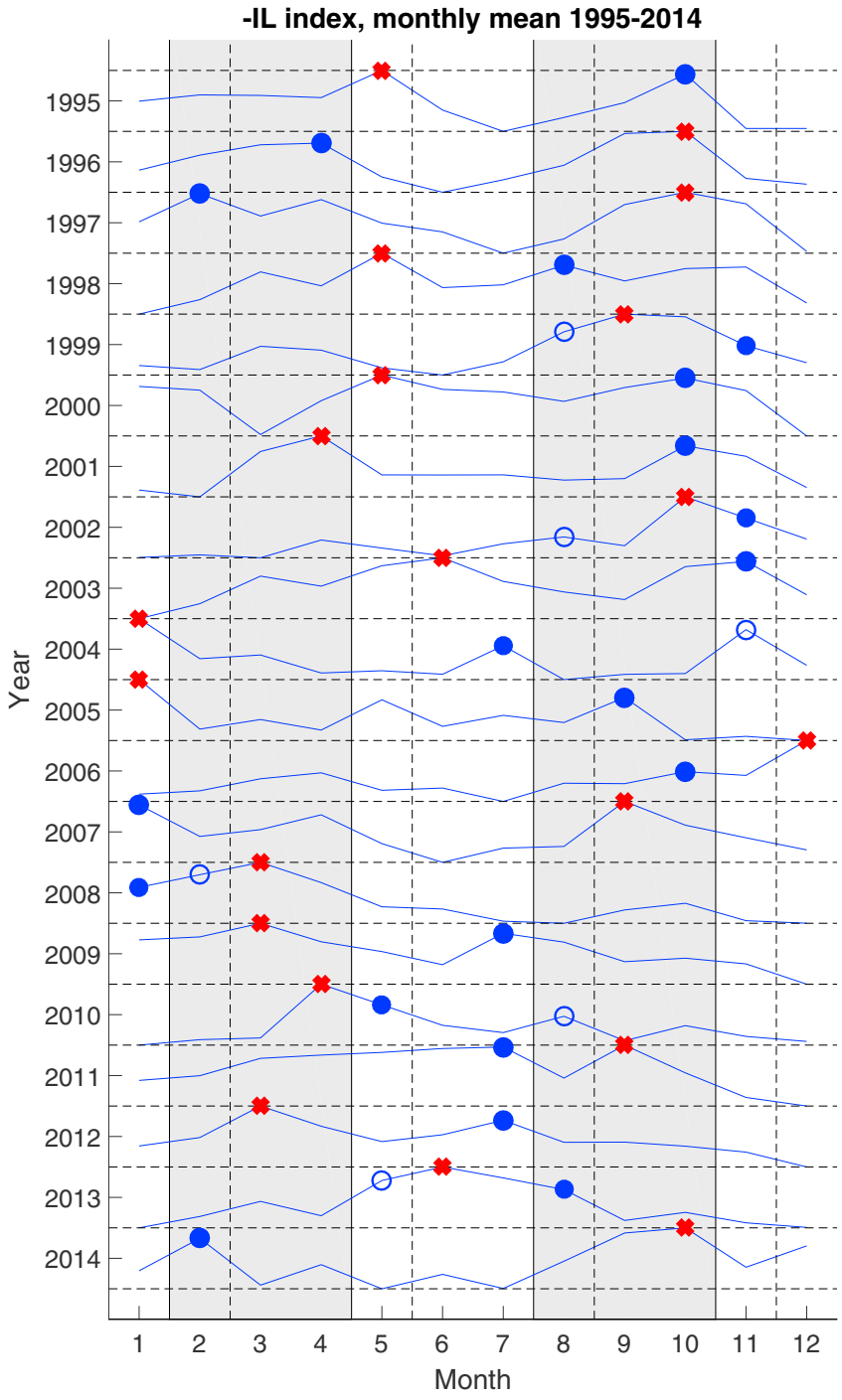

Figure 2. Seasonal variation of the $-IL$ index for each year in 1995–2014 normalized to the same range of variation (y axes). The vertical solid black lines limiting the grey shaded areas denote the boundaries of the seasons by definition 1 (February–April and August–October). The vertical black dashed lines denote the seasons by definition 2 (March–May and September–November). The most active month for each year is marked by a red cross and the second most active month by a blue circle, filled (open) for definition 1 (2) of seasons.

seasonal variation shows the well-known two-equinox maxima pattern (to be called here the EE pattern) (Bartels, 1932; Cortie, 1912; McIntosh, 1959; Mursula et al., 2011; Russell & McPherron, 1973; Zhao & Zong, 2012), with a slightly sharper and more pronounced fall peak in October and a wider spring peak in March–May. Although such long-term superposed means produce the EE pattern, the relative heights of the two peaks as well as their widths and exact peak months vary when the selection of the years

included to the SPE-analysis is varied. Only the SPE curve for 1995–2014 time interval is shown here. The monthly means of *IL* index for individual years are shown later in Figure 2. Overall, the two geomagnetic activity indices used here show very similar solar cycle and seasonal variations, and either one could be used as a measure of high-latitude geomagnetic activity in monthly and yearly time scales.

We use here two different definitions for the seasons. In the tradition of geomagnetic activity studies, one defines the four 3-monthly seasons so that the spring and fall seasons are around the equinox months (February–April and August–October). This is motivated since the leading mechanism producing the EE pattern is the equinoctial mechanism (Cliver et al., 2000; Lyatsky et al., 2001), which is indeed centered at exact equinoxes. We call this here definition 1. However, since Figure 1 shows that the three most active spring months in these indices in 1995–2014 were March–May, we will also use the seasons defined by this result and call it definition 2 of the seasons. In fact, the peaking of geomagnetic activity on the month after the equinox (April and October) is in agreement with the prediction of the Russell-McPherron mechanism (Russell & McPherron, 1973), which also strongly affects the seasonal EE pattern.

The seasonal variation of high-latitude geomagnetic activity in individual years in 1995–2014 is shown in Figure 2 based on the (absolute) monthly values of the *IL* index. Each year is scaled between the annual maximum and minimum to the same extent in Figure 2 in order to better show the seasonal variation irrespective of the amplitude of the yearly variation. The most active month (maximum of $-IL$ index) of each year is marked by a red cross. The month with the second largest activity, which is required to be outside the season of the primary maximum, is marked by a filled blue circle for definition 1 of seasons and by an open blue circle for definition 2. (When they are on the same month, only filled circle shows). For example, in the year 1995, the most active month is May, and thus, this month is marked by a red cross in Figure 2. The second-most active month is October, which is marked by a filled blue circle. The most and second-most active months in 1995 are same for the both season definitions, unlike, for example, in 1999 when the second-most active month according to definition 1 is in November but in August according to definition 2. The second-most active month cannot be in August using definition 1, because then both the most active month (i.e., September) and the second-most active month (i.e., August) would be in the same fall season. The vertical solid black lines limiting the grey shaded areas denote the boundaries of the seasons by definition 1, and the vertical black dashed lines denote the seasons by definition 2.

We will determine in this paper the seasonal pattern of high-latitude geomagnetic activity based on the seasons of the primary and secondary maxima depicted in Figure 2. The seasonal pattern of the year is called equinox-dominated (abbreviated as E), when the dominant season (the season of the primary maximum) is either spring or fall. When the dominant season is summer or winter, the seasonal pattern in that year is solstice-dominated (abbreviated as S). Note that, as described above, some months can represent either equinox or solstice depending on the definition of seasons (definition 1 versus definition 2). Figure 2 can be used to find the dominant season for both of these two definitions. Accordingly, one can find in Figure 2 that when using the season definition 1 (2), there are 8 (5, respectively) solstice-dominated years out of 20 years, that is, in 40% (25%) of all years in 1995–2014.

Similarly, one can determine from Figure 2 the season of the secondary maximum for all years using either season definition (filled or open blue circles). Thereafter, one can specify the seasonal variation of each year to be of either EE, ES, SE, or SS type, where the first letter of the pair denotes the season of the primary maximum and the second letter the secondary maximum. Table 1 collects this information from Figure 2 and lists the seasons of the primary and secondary maxima (according to the *IL* index) for each year in 1995–2014 using this notation. Results for both definitions of seasons are included in Table 1.

Table 1 shows that the two-equinox (EE) seasonal pattern occurs only in four out of 20 years (20%) in 1995–2014 according to both season definitions. (Two of these four years, 1996 and 2001, are the same in both definitions). This small fraction of EE-years implies a dramatically different view about the typical seasonal variation of high-latitude geomagnetic activity in individual years, which is not in agreement with the traditional two-equinox pattern suggested by the superposed epoch pattern (such as in Figure 1). The most common seasonal pattern is the ES type, which is valid in 8 (11) out of 20 years, that is, 40% (55%) of years in 1995–2014 according to definition 1 (2, resp.). Out of the 8 (5) solstice-dominated years, the mixed SE pattern is, with 6 (5) years, by far more common.

Table 1
Equinox (E) and Solstice (S) Location of Primary and Secondary Maxima Based on the IL Index for the Years 1995–2014, Organized to Solar Cycles 22–24 (Column 3), Number of Years With Classical Equinox EE Pattern (Column 4), and Number of Years With Maxima at Either Solstice (SS or SE) (Column 5)

Solar cycle	Year	Seasonal pattern from *IL* index Primary and secondary *IL* maxima	Classical 2-equinox pattern (EE)	Maximum at either solstice (SS or SE)
		Definition 1		
SC22	1995–1996	SE-EE	1/2 (50%)	1/2 (50%)
SC23	1997–2008	EE-SE-ES-SE-EE-ES-SS-SS-SE-SE-ES-ES	2/12 (17%)	6/12 (50%)
SC24	2009–2014	ES-ES-ES-ES-SE-EE	1/6 (17%)	1/6 (17%)
			4/20 (20%)	8/20 (40%)
		Definition 2		
SC22	1995–1996	EE-EE	2/2 (100%)	0/2 (0%)
SC23	1997–2008	ES-ES-ES-EE-EE-ES-SE-SE-SE-SE-ES-ES	2/12 (17%)	4/12 (33%)
SC24	2009–2014	ES-ES-ES-ES-SE-ES	0/6 (0%)	1/6 (17%)
			4/20 (20%)	5/20 (25%)

Note. For example, SE indicates that the primary maximum is in either solstice and the secondary maximum is in either equinox. In definition 1 equinoxes are defined from February to April and from August to October, while in definition 2 from March to May and from September to November.

As discussed above, the multiyear superposed seasonal variation depicted in Figure 1 (right) clearly shows two roughly equally high maxima in spring and fall, that is, the EE pattern. However, the individual years in Table 1 show that in 80% of years, at least one of the two equinox peaks vanishes from among the two highest seasons, leaving typically one equinox, either spring or fall, as a primary or secondary maximum for most years. Thus, while a small number of true two-equinox maxima years also exist, the well-known two-equinox pattern is mainly obtained by combining years with one equinox maximum, alternatingly in spring or fall equinox (see also Mursula et al., 2011). Finally, we would also like to note that, obviously, the multiyear superposed seasonal curve varies slightly, depending on the selection of years superposed.

4. Seasonal Variation of Solar Wind Speed in 1995–2014

Previous studies have shown that solar wind speed is an important driver of long-term (e.g., monthly and yearly) geomagnetic activity at low latitudes and midlatitude (Akasofu, 1981; Crooker, Feynman, & Gosling, 1977; Richardson, Cane, & Cliver, 2002; Richardson, Cliver, & Cane, 2000) and, especially, at high latitudes (Finch et al., 2008; Holappa, Mursula, & Asikainen, 2014; Holappa, Mursula, Asikainen, & Richardson, 2014; Lukianova, Mursula, & Kozlovsky, 2012; Mursula, Holappa, & Lukianova, 2017; Mursula, Lukianova, & Holappa, 2015) and of substorm activity (Tanskanen et al., 2005). Here we study to what extent the solar wind speed controls the seasonal variation of high-latitude geomagnetic activity.

Figure 3 shows the monthly mean values of solar wind speed and the *IL* index (note the inverse axis) on top of each other. The high-latitude geomagnetic activity is seen to closely follow the solar wind speed, both over longer, interannual (solar cycle) time scales, as well as seasonal time scales. The linear correlation coefficient between the monthly values of the *IL* index and solar wind speed is 0.817 ($p < 1.5 * 10^{-44}$). The highest monthly values of solar wind speed, over 600 km/s, are found in 2003. The largest monthly disturbances are also found at the same time (monthly *IL* indices of about −150 nT). Note that while OMNI database has, in general, a good coverage over the studied time interval, it misses some hours of data, for example, during the CME of October 2003. However, even if the October *IL* values include the CME effects, the highest monthly means are found earlier in 2003. The lowest values of both solar wind speed and the *IL* index are observed at the end of 2009 (300 km/s and −20 nT, respectively). Accordingly, Figure 3 shows that the *IL* index (high-latitude geomagnetic activity, more generally) reasonably follows the solar wind speed even at monthly time scales, so suggesting for at least a fair agreement for the seasonal variation of individual years between these two parameters.

This is studied further in Figure 4, which depicts the seasonal variation of solar wind speed for individual years in 1995–2014 using the same format as in Figure 2 for the *IL* index. Solar wind speed for each year is scaled between the annual maximum and minimum in order to better show the seasonal variation, irrespective of the amplitude of the yearly variation, in a same way as was done in Figure 2. The month with the highest value of solar wind speed of each year is marked by a black cross in Figure 4. The month with the second

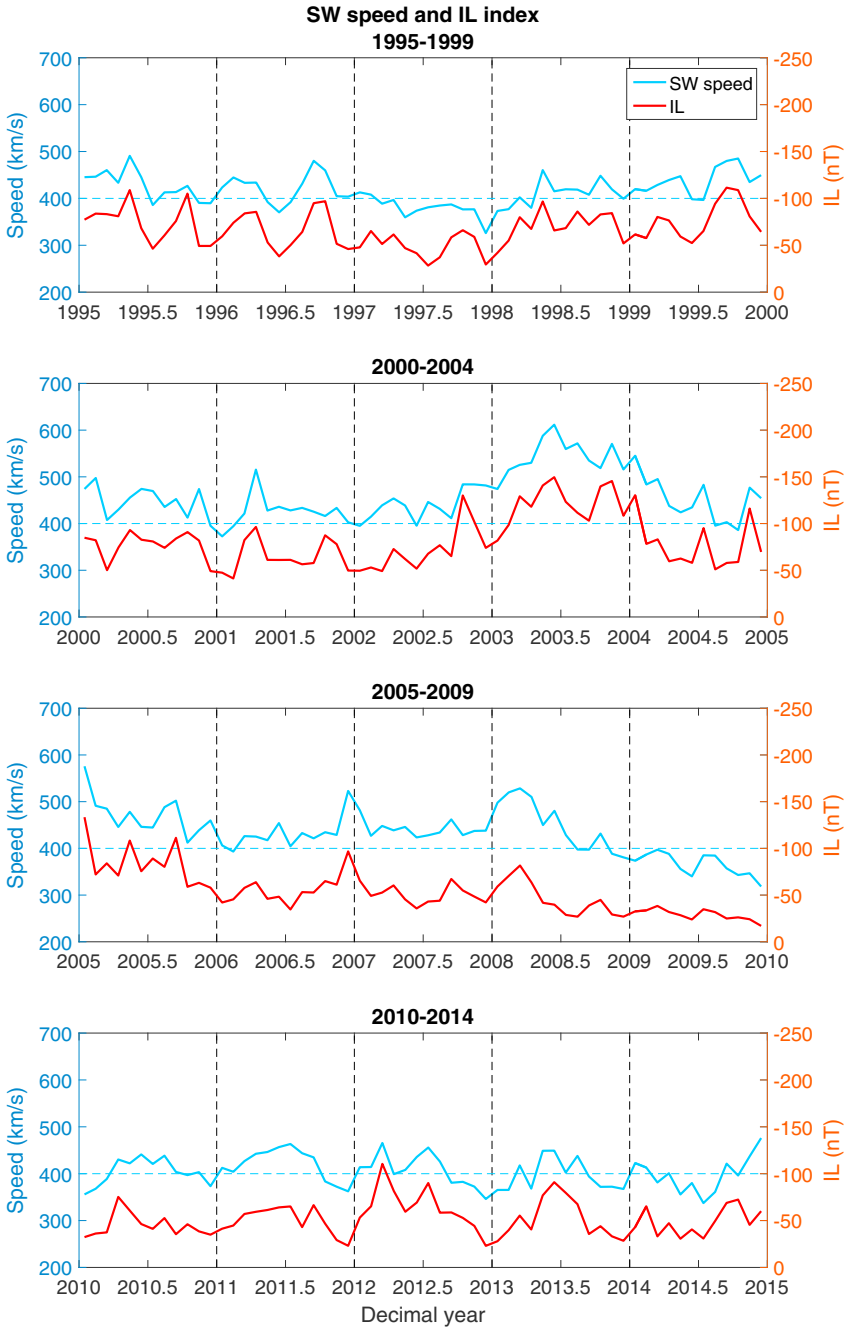

Figure 3. Monthly averages of *IL* index (red line) together with solar wind speed (turquoise line) for the years 1995–2014. The vertical dashed line marks the 400 km/s and −100 nT thresholds.

highest speed (outside the season of the primary maximum) is marked by a green filled circle for definition 1 of seasons and by an open green circle for definition 2. The corresponding seasonal patterns (EE, ES, SE, and SS) of the primary and secondary annual maxima of solar wind speed are given in Table 2 for each year. Note that the patterns are the same in solar wind speed and the *IL* index in 10 (9) out of 20 years for definition 1 (2) of seasons. This is far beyond random chance. Assuming equal distribution of all four patterns (which is, of course, not strictly valid) and using binomial cumulative distribution, one would get 10 (9) or more similar patterns by random fluctuation at the probability of 0.4% (1.4%) only.

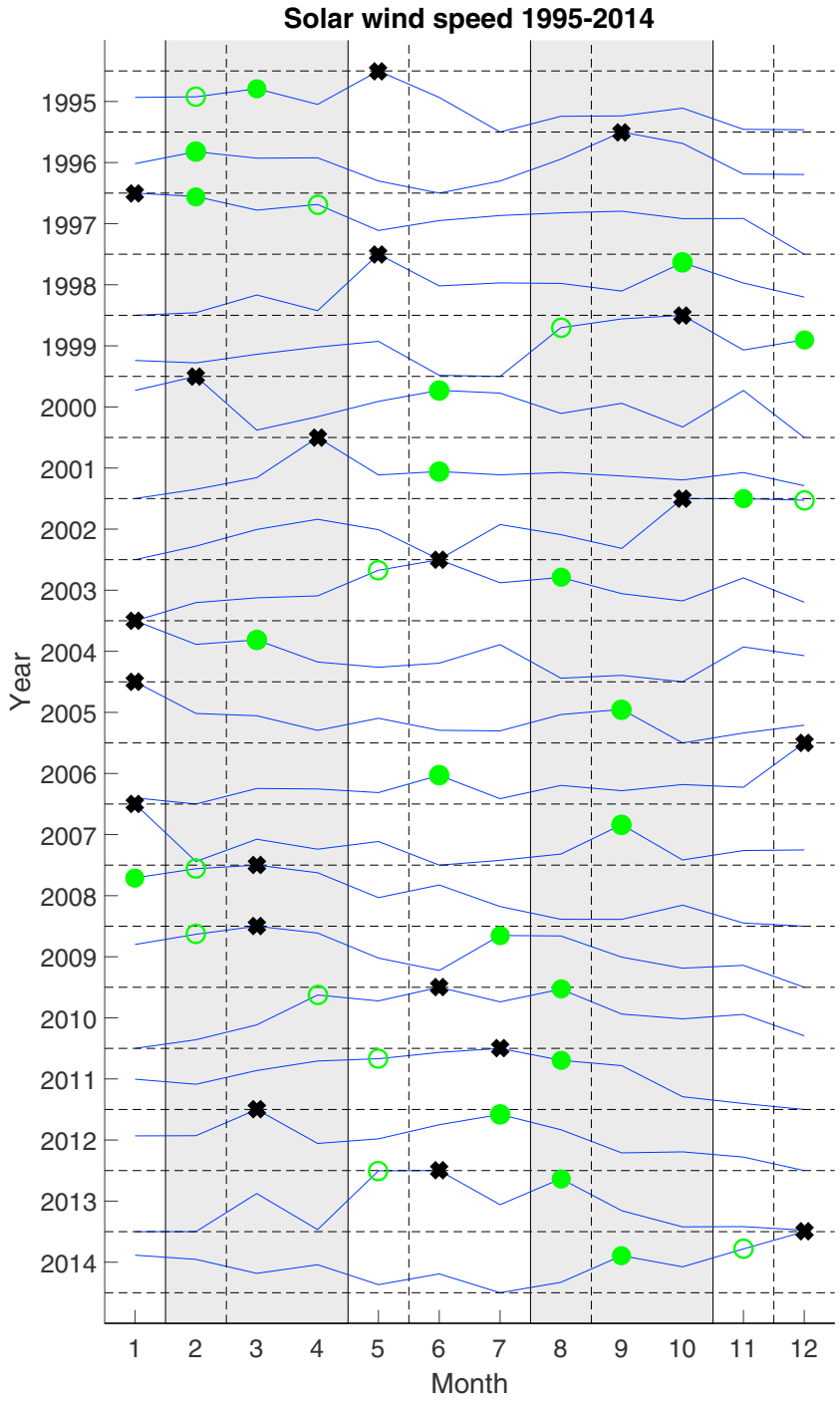

Figure 4. Same as Figure 2 but for solar wind speed. The most active month for each year is marked by a black cross and the second most active month by a green circle, filled (open) for definition 1 (2) of seasons.

Figure 5 presents another comparison of the seasonal variation in solar wind speed and the *IL* index. Figure 5 (top) shows the months of the primary and secondary maxima of the *IL* index for each year in 1995–2014. Figure 5 (middle and bottom) compare the months of the primary (middle) and secondary (bottom) maxima solar wind speed and the *IL* index. The primary maxima of solar wind speed and the *IL* index are in the same season (out of four seasons) in 14 out of 20 years (70%) for both definitions of seasons. Using binomial cumulative distribution, the probability for having the same season in *IL* and SW speed during 14 or more years out

Table 2
Same as Table 1 but for the Solar Wind Speed

Solar cycle	Year	Seasonal pattern from solar wind speed Primary and secondary maxima	Classical 2-equinox pattern (EE)	Maximum at either solstice (SS or SE)
		Definition 1		
SC22	1995–1996	ES-SE	0/2 (0%)	1/2 (50%)
SC23	1997–2008	EE-ES-SS-ES-ES-SE-SE-SE-SS-SE-ES	1/12 (8%)	6/12 (50%)
SC24	2009–2014	ES-SE-SE-ES-SE-SE	0/6 (0%)	4/6 (67%)
			1/20 (5%)	11/20 (55%)
		Definition 2		
SC22	1995–1996	ES-EE	1/2 (50%)	0/2 (0%)
SC23	1997–2008	SE-SE-ES-ES-ES-ES-SE-SE-SE-SS-SE	0/12 (0%)	7/12 (58%)
SC24	2009–2014	ES-ES-SE-SE-ES-SE-SE	0/12 (0%)	4/12 (33%)
			1/20 (5%)	11/20 (55%)

of 20 due to random fluctuations is only $4 * 10^{-6}$. In fact, the primary maxima of *IL* and solar wind speed are at the same month in 12 out of 20 years (60%), which gives even a lower probability of random occurrence of only $5 * 10^{-10}$. In those years when the seasons of the primary maxima of *IL* and solar wind speed disagreed, the secondary maximum of *IL* index was found in the primary maximum season of solar wind speed in almost all years.

Let us still study the equinox-solstice division of years according to the primary and secondary maxima of the solar wind speed. There are 8 (9) equinox-dominated and 12 (11) solstice-dominated years in the seasonal variation of solar wind speed according to definition 1 (2) of seasons (see Table 2). Thus, the solar wind speed

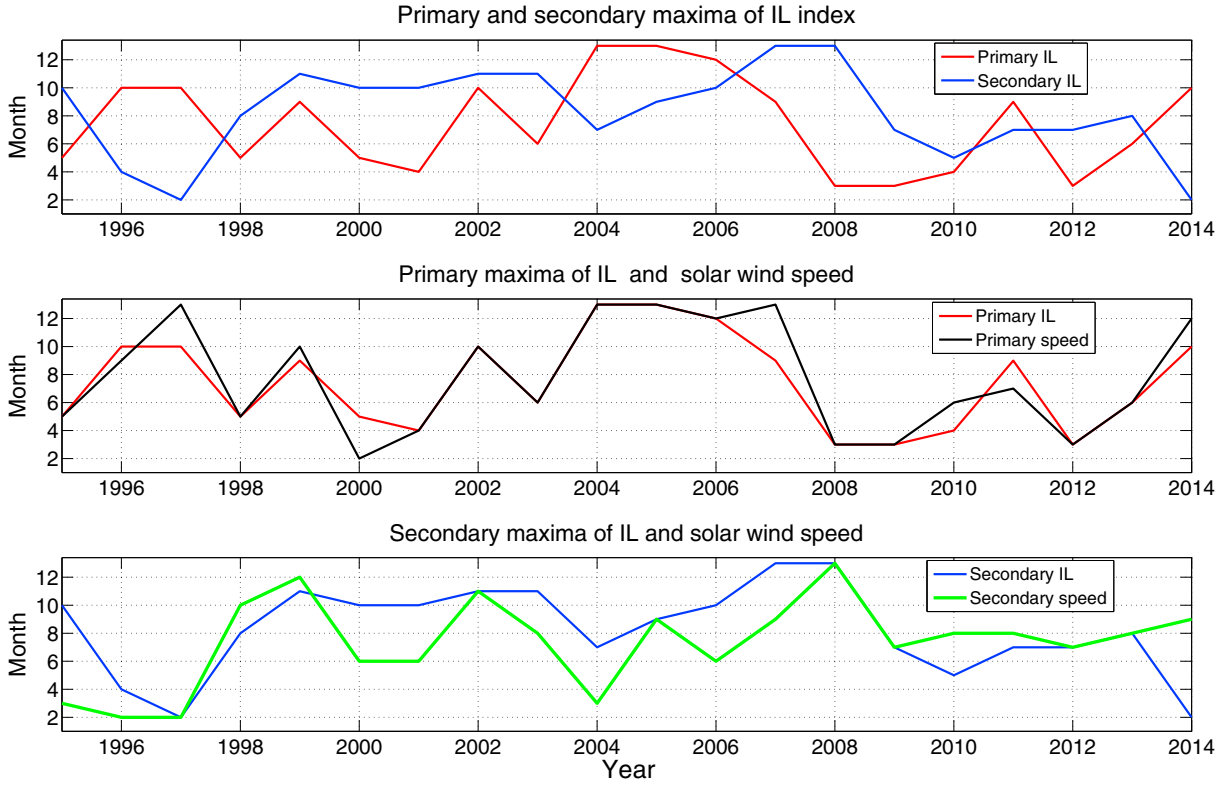

Figure 5. (top) Month of primary (red) and secondary (blue) maxima of the $-IL$ index in each year. (middle) Month of primary maxima of $-IL$ index (red) and primary maxima of solar wind speed (black). (bottom) Month of secondary maxima of $-IL$ index (blue) and secondary maxima of solar wind speed (green). January is shown on top of December (i.e., located at month number 13) in each panel for continuity of the winter season.

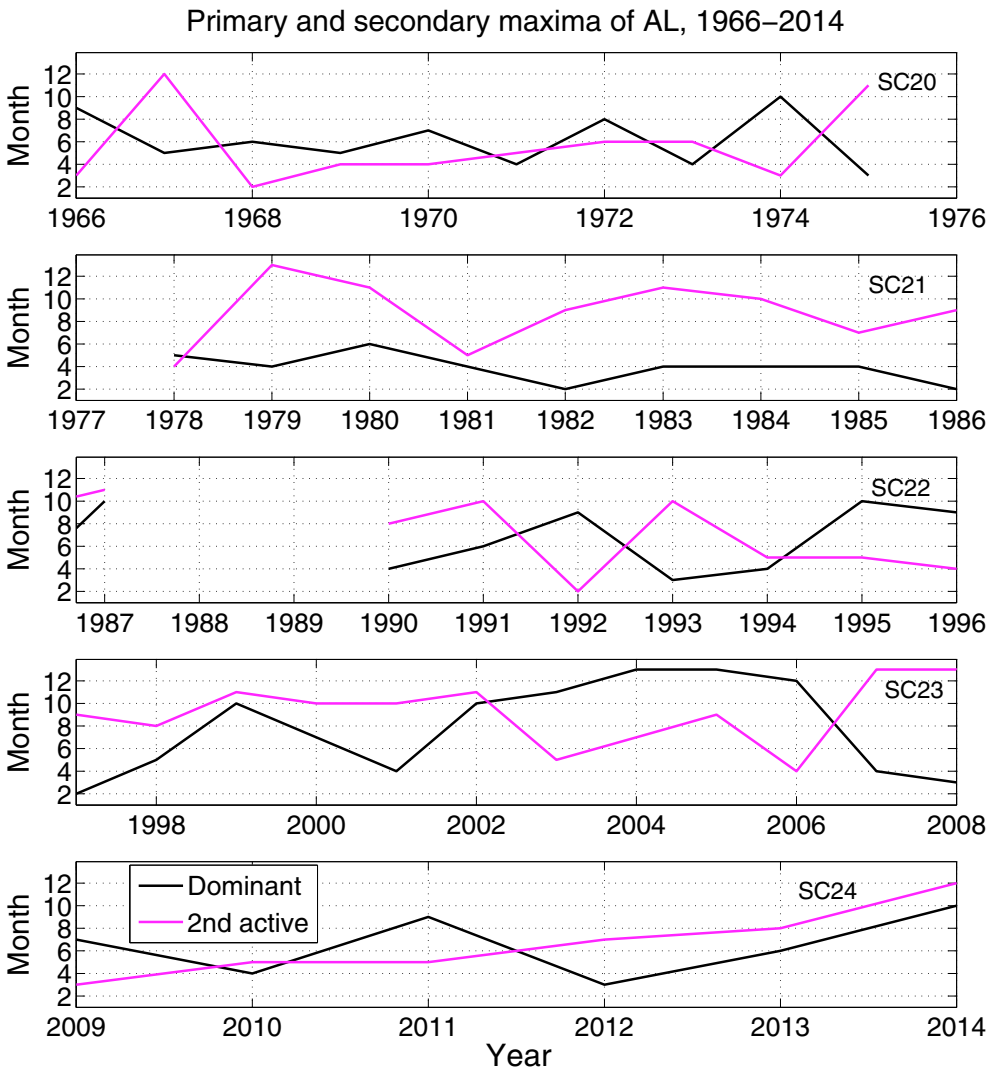

Figure 6. Month of primary (black) and the secondary (pink) seasonal maxima of $-AL$ index since 1966. January is shown on top of December (i.e. located at month number 13) in each panel.

maxima occur relatively more often at the solstices compared to the *IL* index (see above and Table 1). There is only 1 (1) EE year and 7 (8) ES years among the equinox-dominated years and 1 (2) SS year and 11 (9) SE years among the 12 (11) solstice-dominated years according to definition 1 (2). The smaller overall number of equinox months as primary or secondary maxima in solar wind speed compared to the *IL* index gives indirect evidence for the action of those factors, like the equinoctial mechanism (Cliver et al., 2000; Lyatsky et al., 2001; Newell et al., 2002) and the Russell-McPherron mechanism (Russell & McPherron, 1973) that are known to increase geomagnetic activity at equinoxes compared to solstices.

We would also like to note that even though the long-term averages (e.g., monthly means) of high-latitude indices, like the *IL* index, are mainly driven by high-speed streams, they are also somewhat affected by transients like coronal mass ejections (see, e.g., Holappa, Mursula, & Asikainen, 2014, Holappa, Mursula, Asikainen, & Richardson, 2014). However, the seasonal variation of high-latitude indices based on the monthly values is predominantly determined by high-speed streams. Only in very few months, mainly in some sunspot maximum years when the HSS activity may be rather weak, the transients have a sufficiently large contribution to monthly values to modify the seasonal variation in that year. For example, the largest storms during the studied interval occurred in October and November 2003 and were caused by strong CMEs. Still, in 2003 the annual maximum of the *IL* index was found in June (see Figure 2) due to persistent high-speed streams.

Table 3
Same as Table 1 but for the AL Index for the Years 1966–2014, i.e., solar cycles 20–24

Solar cycle	Years	Seasonal pattern from *AL* index Primary and secondary maxima	Classical 2-equinox pattern (EE)	Maximum at either solstice(SS or SE)
		Definition 1		
SC20	1966–1976	EE–SS–SE–SE–SE–ES–ES–ES–EE–ES-NA	2/10 (20%)	4/10 (40%)
SC21	1977–1986	NA–SE–ES–SS–ES–EE–ES–EE–ES-EE	3/9 (33%)	2/9 (22%)
SC22	1987–1996	ES-NA-NA–EE–SE–EE–EE–ES–ES-EE	4/8 (50%)	1/8 (13%)
SC23	1997–2008	EE–SE–ES–SE–EE–ES–SS–SS–SE–SE–ES–ES	2/12 (17%)	6/12 (50%)
SC24	2009–2014	SE–ES–ES-ES-SE-ES	0/6 (0%)	2/6 (33%)
SC20–24	1966–2014		11/45 (24%)	15/45 (33%)
		Definition 2		
SC20	1966–1976	EE–ES–SS–EE–SE–ES–SE–ES–EE–EE-NA	4/10 (40%)	3/10 (30%)
SC21	1977–1986	NA–ES–ES–SE–EE–SE–ES–EE–ES-SE	2/9 (22%)	3/9 (33%)
SC22	1987–1996	ES-NA-NA–ES–SE–ES–EE–ES–EE-EE	3/8 (38%)	1/8 (13%)
SC23	1997–2008	SE–ES–ES–SE–EE–ES–EE–SE–SE–SE–ES–ES	2/12 (17%)	5/12 (42%)
SC24	2009–2014	SE–ES–EE-ES-SE-ES	1/6 (33%)	2/6 (33%)
SC20–24	1966–2014		12/45 (27%)	14/45 (32%)

Note. NA marks a year when data are not available.

Moreover, the secondary maximum of the *IL* index in 2003, which was in November, was also due to HSSs, not to CMEs. In fact, even after removing the storm periods out of the monthly mean, November remains as the secondary maximum month of the *IL* index in 2003.

5. Seasonal Variation of *AL* in Solar Cycles 20–24

We will now extend our study of the seasonal variation of high-latitude geomagnetic activity to cover years from 1966 to 2014 by using the *AL* index (Davis & Sugiura, 1966), which is produced at the World Data Center in Kyoto. This period covers the solar cycles (SC) 20–23 and half of the ongoing SC24. Our aim is to examine the possible change of the seasonal pattern over this long time interval and possible differences between the included solar cycles.

Figure 6 shows the primary and the secondary maximum months for the *AL* index since 1966 (note the data gaps in 1976–1977 and 1988–1989). Each solar cycle (from solar minimum to the next) is depicted in Figure 6 in its own panel. Figure 6 shows that the seasonal patterns for the five solar cycles differ from each other and that the classical two-equinox pattern occurs rather seldom. Table 3 depicts these features even more quantitatively, listing the equinox-solstice (E/S) classification according to the primary and secondary maxima of the *AL* index for all individual years since 1966, in the same way as given in Tables 1 and 2 for the *IL* index and solar wind speed in 1995–2014.

The seasonal pattern of solar cycle 20 (SC20) in Figure 6 shows that summer is the primary maximum season for roughly one third of the years (4 out of 10 for definition 1 and 3 out of 10 for definition 2), mainly in the ascending phase of the cycle, while the rest of the cycle is mostly dominated by either equinox. Overall, during SC20 there are 6 (7) equinox-dominated (EE or ES) and 4 (3) solstice-dominated (SE or SS) years according to definition 1 (2). The classical two-equinox pattern was seen in 20% (40%) of the years using definition 1 (2).

The seasonal pattern of SC21 differs greatly from SC20. The typical feature for SC21 is the strong spring dominance of the primary maximum, which is found in 7 (6) out of 9 years for definition 1 (2). Not once is the primary maximum found in the fall equinox. There are 2 (3) solstice-dominated years during SC21, and the two-equinox pattern is seen in 3 (2) years.

Solar cycle 22 is the only cycle, where the two-equinox pattern dominates. (Unfortunately, data for two years of the ascending phase is missing). Indeed, the EE pattern is found in 4 (3) out of 8 years, that is, in 50% (38%). There was only one solstice-dominated year during this cycle, leading to the lowest fraction (13%) among the studied five cycles. The solstice-dominated year was 1991, that is, close to the maximum of the cycle. We also note that there were only 4 (5) out of 16 cases where a primary or secondary maximum was found in solstice. This fraction of 25% (32%) is also the lowest found in this study.

The seasonal pattern of SC23 is again different from the three previous cycles. The fraction of solstice-dominated years during SC23, 6 (5) out of 12 for definition 1 (2) is the largest in this study. The unique feature for SC23 is the period of 4 (3) consecutive years of winter dominance, 2003–2006 for definition 1 (2004–2006 for definition 2). We note that there were only very few winter-dominated years in the *AL* index since 1966 before this interval (none in definition 1, three in definition 2) and none in the eight studied years after 2006 according to either definition. The probability that the number of winter-dominated years was as small as 4–5 or smaller only due to random fluctuations is highly improbable ($p = 0.2\%$ for definition 1 and $p = 0.8\%$ for definition 2). Also, the random occurrence of 3–4 consecutive winter years is very improbable ($p = 0.4\%$ for definition 1 and $p = 1.6\%$ for definition 2).

For SC24 our results only cover the ascending phase and solar maxima. Therefore, the results for this cycle are not quite comparable with the more complete cycles. Anyway, the fraction of solstice-dominated years during SC24 (33%) and the fraction of solstice as a primary or secondary maximum (50% for definition 1 and 42% for definition 2) are quite high. The two-equinox pattern in solar cycle 24 was not found at all for definition 1, and only once in six years for definition 2, while the overall occurrence of the EE pattern was 11 (12) during the 45 year time interval included, that is, in 24% (27%) of years for definition 1 (2). We note that the numbers for SC24 are still preliminary, and the declining phase may well raise the relative fraction of equinox years.

6. Discussion

The seasonal variation of geomagnetic activity has typically been studied in terms of superposing the variation from several years, which leads to the well-known two-equinox pattern depicted in Figure 1 (right). Several mechanisms have been proposed to explain this semiannual pattern, including the equinoctial effect, the Russell-McPherron effect, and the axial effect due to the Earth's varying heliographic latitude. However, very few papers have studied the seasonal variation in individual years or compared the variation in different solar cycles (Mursula et al., 2011; Tanskanen et al., 2011).

In this paper we have studied the seasonal variation of high-latitude geomagnetic activity in individual years by using two auroral electrojet indices, the *IL* index in 1995–2014 and *AL* index in 1966–2014. We used two definitions for the seasons: definition 1 corresponding more closely to the seasonal variation of the equinoctial effect and definition 2 to the Russell-McPherron effect. We have shown that independent of season definition, one of the two equinoxes dominates the seasonal variation in two thirds of the years in 1966–2014. In the remaining years the annual maximum occurs during either solstice, more often during summer than in winter. However, only in 11 (12) out of 45 years, that is, in roughly one fourth of the years, the seasonal pattern is following the two-equinox maxima pattern of the superposed seasonal variation.

Accordingly, it is clear that the two-equinox pattern is not the dominant, not even the most common seasonal pattern in individual years, contrary to the impression obtained when combining the seasonal variation over a number of years. However, this result does not mean that processes such as the equinoctial and the Russell-McPherron mechanisms that contribute to enhance geomagnetic activity at equinoxes over solstices are not operating. Moreover, as we have shown in this paper, the relative fraction of the four different seasonal patterns varies in time (e.g., between solar cycles), and the EE pattern can sometimes, most clearly during the declining phase of solar cycle 22, be the dominant pattern of seasonal variation in high-latitude geomagnetic activity.

It is known since long that solar wind speed is the main driver of long-term averaged values of geomagnetic activity at high latitudes (Clauer et al., 1981; Holzer & Slavin, 1982; Bargatze, 1985). We have also shown this close connection in this paper in several ways. Using monthly values, the correlation between solar wind speed and the *IL* index in 1995–2014 is excellent ($cc = 0.817$; $p < 1.5 * 10^{-44}$), and solar wind speed alone explains two thirds ($cc^2 = 0.668$) of the variability of the *IL* index at monthly resolution. This excellent correlation between solar wind speed and the *IL* index is shown here to also lead to an excellent agreement between their seasonal variation patterns during individual years. We noted that the annual maxima of solar wind speed and the *IL* index occur in the same month in 12 out of 20 years (60%), which is found randomly only at a very low probability of about $5 * 10^{-10}$. Moreover, we found that irrespective of season definition, the annual maxima of solar wind speed and the *IL* index are in the same season in 14 out of 20 years (70%), which takes place randomly is only at a probability of $4 * 10^{-6}$.

Despite this good agreement between the seasonal patterns of solar wind speed and high-latitude geomagnetic activity in individual years, there is a tendency that the seasonal pattern of high-latitude geomagnetic activity is somewhat more inclined toward equinoxes than solar wind speed. Indeed, while there are 8 (9) equinox-dominated and 12 (11) solstice-dominated years in 1995–2014 in the seasonal variation of solar wind speed according to definition 1 (2) of seasons (see Table 2), there are 12 (15) equinox-dominated and 8 (5) solstice-dominated years in the *IL* index. Moreover, there is only one two-equinox year in solar wind speed but four in the *IL* index in 1995–2014. The smaller overall number of equinox months as primary or secondary maxima in solar wind speed compared to the *IL* index further support the view that also other factors than the solar wind speed, in particular the equinoctial mechanism (Cliver et al., 2000; Lyatsky et al., 2001; Newell et al., 2002) and the Russell-McPherron mechanism (Russell & McPherron, 1973), contribute to increase geomagnetic activity at equinoxes over solstices.

We also made an extended study by examining the properties of the seasonal variation in the *AL* index during five solar cycles (SC20–SC24). Comparing the occurrence of the different seasonal patterns, we found interesting long-term changes and differences between the solar cycles. The equinox dominance of the annual (primary) maximum is first found to increase from roughly 60–70% (depending on season definition) for SC20 to 80–90% for SC22, and then to drop to a lower level of 50–60% in cycle 23 (see Table 3). Similarly, the fraction of the two-equinox (EE) pattern increases from the level 20–40% for SC20 to 50–63% in SC22, and then drops back to a lower level of about 15–20% in SC23. These changes are related to the long-term evolution of solar magnetic fields, in particular to the evolution of polar coronal holes and to the strength of solar polar fields, which control the properties of the solar wind and the heliospheric current sheet (HCS). When the solar polar fields are strong, like in the late declining to minimum phase of SC21 and SC22 (Lockwood & Owens, 2011; Munoz-Jaramillo et al., 2012; Wang, 2016), strong heliolatitudinal gradients of solar wind speed are formed around the HCS at low heliographic latitudes (Tokumaru et al., 2009). These gradients increase the occurrence of high-speed solar wind streams during the Earth's high-latitude times in September and March, leading to higher geomagnetic activity at these times. This contributes to the fairly large number of equinox-dominated years during the declining phase of SC21 (1982–1986) and SC22 (1991–1996). In fact, these two declining phases include a sizable fraction of all EE years.

On the other hand, during SC23, the solar polar fields dramatically weakened (Smith & Balogh, 2008), making the HCS wider (Mursula & Virtanen, 2011) and reducing heliolatitudinal gradients at low heliolatitudes (e.g., around the ecliptic). Moreover, a large persistent coronal hole appeared at low latitudes in the southern hemisphere in 2003 (Abramenko et al., 2010; Gibson et al., 2009; Ko et al., 2014), which increased the solar wind speed during solstice times. We note that the highest monthly solar wind speeds in 1995–2014 were found in June 2003, as seen in Figure 3. High values of solar wind speed were found in subsequent winters, especially in winter 2003/2004, 2004/2005, and 2006/2007 (see Figure 3). The related modified seasonal distribution of solar wind speed is the reason for the exceptional winter solstice dominance of the primary seasonal maximum of the *AL* index in 2004–2006 (see Figure 6) and in solar wind speed in 2004–2007 (see Figure 3, middle). As shown here, the chain of winter-dominated years is highly improbable to be caused by random fluctuations. The modified distribution of solar wind speed also explains why no EE years occurred during SC23 after 2003, although the late declining phase of the cycle normally has the best conditions for the two-equinox maxima pattern, as was seen in cycles 21 and 23.

7. Conclusions

We have studied here the seasonal variation of high-latitude geomagnetic activity in individual years in 1995–2014 using the *IL* index and in 1966–2014 using the *AL* index. We have identified the most active (primary) and the second most active (secondary) season for each year based on these indices. We have found that overall in the last four and half solar cycles (45 years), only less than one third of the individual years depict the classical two-equinox maximum pattern, which is based on superposing seasonal patterns over many years. The annual maximum is found to be located in either equinox in two thirds of the individual years examined and at either solstice in one third of the years.

We have confirmed the earlier finding of the close connection between solar wind speed and high-latitude geomagnetic activity, showing that solar wind speed explains two thirds of the variability of high-latitude

geomagnetic activity at the monthly resolution. This confirms that solar wind speed is the main long-term driver of high-latitude geomagnetic activity.

Moreover, we have shown that the seasonal variation of high-latitude geomagnetic activity follows the seasonal pattern solar wind speed in a large fraction of individual years, in many more years than can be obtained by statistical fluctuations. However, there is a tendency for the seasonal variation in geomagnetic activity to favor equinoxes slightly more than the seasonal variation of solar wind speed. This suggests that the well-known mechanisms, like the equinoctial mechanism and the Russell-McPherron mechanism, also contribute to the seasonal variation of geomagnetic activity.

However, the long-term change of solar wind speed, due to the corresponding long-term changes in solar coronal holes, often mask the effect of these mechanisms for individual years. Therefore, the seasonal variation of high-latitude geomagnetic activity in individual years does not often reproduce the two-equinox maximum pattern that is obtained when superposing several years.

We found significant differences in the typical seasonal pattern between the five solar cycles studied, as a response to the long-term evolution of solar coronal holes. Most dramatically, this evolution shows up in the fraction of equinox primary years, as well in the fraction of the two-equinox pattern, which both increased from SC20 to a maximum during SC22, and then dropped back to a lower level during SC23. During solar cycle 23 we also found a rare sequence of winter solstice-dominated years, due to high-speed solar wind streams emerging from the low-latitude solar coronal hole persisting for many years in declining phase of cycle 23.

Acknowledgments
We wish to thank the institutes maintaining the IMAGE magnetometer network. The IMAGE magnetic field measurements are available at http://space.fmi.fi/image/beta/ and *IL* indices at http://space.fmi.fi/image/il_index/ and at http://www.substormzoo.org. We thank Kyoto World Data Center for producing the *AL* indices for 1966–2014 and NSSDC OMNI2 database for providing the solar wind velocity observations. We acknowledge the financial support by the Academy of Finland to the ReSoLVE Centre of Excellence (project 272157).

References

Abramenko, V., Yurchyshyn, V., Linker, J., Mikic, Z., Luhmann, J., & Lee, C. O. (2010). Low-latitude coronal holes at the minimum of the 23rd solar cycle. *The Astrophysical Journal*, *712*, 813–818.

Akasofu, S.-I. (1981). Energy coupling between the solar wind and the magnetosphere. *Space Science Reviews*, *28*, 121.

Bargatze, L. F. (1985). Magnetospheric inpulse response for many levels of geomagnetic activity. *Journal of Geophysical Research*, *90*, 6387.

Bartels, J. (1932). Terrestrial-magnetic activity and its relation to solar phenomena. *Terrestrial Magnetism and Atmospheric Electricity*, *37*, 1.

Birkeland, K. (1908). *The Norwegian Aurora Polaris Expedition 1902–1903* (Vol. 1, 1st Sect). Norway, Oslo: Aschhoug.

Clauer, C. R., McPherron, R. L., Searls, C., & Kivelson, M. G. (1981). Solar wind control of auroral zone geomagnetic activity. *Geophysical Research Letters*, *8*, 915.

Cliver, E. W., Kamide, Y., & Ling, A. G. (2000). Mountains versus valleys: Semiannual variation of geomagnetic activity. *Journal of Geophysical Research*, *105*(A2), 2413–2424.

Clúa de Gonzales, A. L., Silbergleit, V. M., Gonzales, W. D., & Tsurutani, B. T. (2001). Annual variation of geomagnetic activity. *Journal of Atmospheric and Terrestrial Physics*, *63*(4), 367.

Cortie, A. L. (1912). Sunspots and terrestrial magnetic phenomena, 1898–1911: The cause of the annual variation in magnetic disturbances. *Monthly Notices of the Royal Astronomical Society*, *73*, 52–60.

Crooker, N., Feynman, J., & Gosling, J. T. (1977). On the high correlation between long-term averages of solar wind speed and geomagnetic activity. *Journal of Geophysical Research: Solar Physics*, *82*, 1933–1937.

Currie, R. G. (1966). The geomagnetic spectrum: 40 days to 5.5 years. *Journal of Geophysical Research*, *71*, 4579.

Davis, T. N., & Sugiura, M. (1966). Auroral electrojet activity index *AE* and its universal time variation. *Journal of Geophysical Research*, *71*, 785.

Finch, I. D., Lockwood, M. L., & Rouillard, A. P. (2008). Effects of solar wind magnetosphere coupling recorded at different geomagnetic latitudes: Separation of directly-driven and storage/release systems. *Geophysical Research Letters*, *35*, L21105. https://doi.org/10.1029/2008GL035399

Gibson, S. E., Kozyra, J. U., de Toma, G., Emery, B. A., Onsager, T., & Thompson, B. J. (2009). If the Sun is so quiet, why is the Earth ringing? A comparison of two solar minimum intervals. *Journal of Geophysical Research*, *114*, A09105. https://doi.org/10.1029/2009JA014342

Holappa, L., Mursula, K., & Asikainen, T. (2014). A new method to estimate annual solar wind parameters and contributions of different solar wind structures to geomagnetic activity. *Journal of Geophysical Research*, *119*, 9407–9418. https://doi.org/10.1002/2014JA020599

Holappa, L., Mursula, K., Asikainen, T., & Richardson, I. G. (2014). Annual fractions of high-speed streams from principal component analysis of local geomagnetic activity. *Journal of Geophysical Research, Space Physics*, *119*, 4544–4555. https://doi.org/10.1002/2014JA019958

Holzer, R. E., & Slavin, J. A. (1982). An evaluation of three predictors of geomagnetic activity. *Journal of Geophysical Research*, *87*, 2558.

Kallio, E. I., Pulkkinen, T. I., Koskinen, H. E. J., Viljanen, A., Slavin, J. A., & Ogilvie, K. (2000). Loading-unloading processes in the nightside ionosphere. *Geophysical Research Letters*, *27*(11), 1627.

Ko, Y.-K., Muglach, K., Wang, Y.-M., Young, P. R., & Lepri, S. T. (2014). Temporal evolution of solar wind ion composition and their source coronal holes during the declining phase of cycle 23. I. Low-latitude extension of polar coronal holes. *The Astrophysical Journal*, *787*, 121.

Lockwood, M., & Owens, M. J. (2011). Centennial changes in the heliospheric magnetic field and open solar flux: The consensus view from geomagnetic data and cosmogenic isotopes and its implications. *Journal of Geophysical Research*, *116*, A04109. https://doi.org/10.1029/2010JA016220

Lukianova, R., Mursula, K., & Kozlovsky, A. (2012). Response of the polar magnetic field intensity to the exceptionally high solar wind streams in 2003. *Geophysical Research Letters*, *39*, L04101. https://doi.org/10.1029/2011GL050420

Lyatsky, W., Newell, P. T., & Hamza, A. (2001). Solar illumination as cause of the equinoctial preference for geomagnetic activity. *Geophysical Research Letters*, *28*(12), 2353.

McIntosh, D. H. (1959). On the annual variation of magnetic field disturbances. *Philosophical Transactions of the Royal Society of London. Series A*, *251*, 525–552.

McPherron, R. L., Hsu, T. S., & Chu, X. (2015). An optimum solar wind coupling function for the *AL* index. *Journal of Geophysical Research*, *120*(4), 2494–2515. https://doi.org/10.1002/2014JA020619

Munoz-Jaramillo, A., Sheeley, N. R. Jr., Zhang, J., & DeLuca, E. E. (2012). Calibrating 100 years of polar faculae measurements: Implications for the evolution of the heliospheric magnetic field. *The Astrophysical Journal*, *753*, 146. https://doi.org/10.1088/0004-637X/753/2/146

Mursula, K., Holappa, L., & Lukianova, R. (2017). Seasonal solar wind speeds for the last 100 years: Unique coronal hole structures during the peak and demise of the Grand Modern Maximum. *Geophysical Research Letters*, *44*, 30–36. https://doi.org/10.1002/2016GL071573

Mursula, K., Lukianova, R., & Holappa, L. (2015). Occurrence of high-speed solar wind streams over the Grand Modern Maximum. *The Astrophysical Journal*, *801*, 30. https://doi.org/10.1088/0004-637X/801/1/30

Mursula, K., Tanskanen, E. I., & Love, J. J. (2011). Spring-fall asymmetry of substorm strength, geomagnetic activity and solar wind: Implications for semiannual varaiation and solar hemispheric asymmetry. *Geophysical Research Letters*, *38*, L06104. https://doi.org/10.1029/2011GL046751

Mursula, K., & Virtanen, I. I. (2011). The last dance of the Bashful Ballerina? *Astronomy and Astrophysics*, *525*, L12. https://doi.org/10.1051/0004-6361/2009139752010

Newell, P. T., Sotirelis, T., Skura, J. P., Meng, C.-I., & Lyatsky, W. (2002). Ultraviolet insolation drives seasonal and diurnal space weather variations. *Journal of Geophysical Research*, *107*(A10), 1305. https://doi.org/10.1029/2001JA000296

Richardson, I. G., Cane, H. V., & Cliver, E. W. (2002). Sources of geomagnetic activity during nearly three solar cycles (1972–2000). *Journal of Geophysical Research*, *107*, 1187.

Richardson, I. G., Cliver, E. W., & Cane, H. V. (2000). Sources of geomagnetic activity over the solar cycle: Relative importance of coronal mass ejections, high-speed streams, and slow solar wind. *Journal of Geophysical Research*, *105*(A8), 18203.

Russell, C. T., & McPherron, R. L. (1973). Semiannual variation of geomagnetic activity. *Journal of Geophysical Research*, *78*, 92–108.

Sabine, E. (1856). On periodical laws discoverable in the mean effects of the larger magnetic disturbances, III. *Philosophical Transactions. Royal Society of London*, *142*, 103–124.

Smith, E. J., & Balogh, A. (2008). Decrease in heliospheric magnetic flux in this solar minimum: Recent Ulysses magnetic field observations. *Geophysical Research Letters*, *35*, L22103. https://doi.org/10.1029/2008GL035345

Syrjäsuo, M. T., Pulkkinen, I., Pellinen, R. J., Janhunen, P., Kauristie, K., Viljanen, A., … Thomas, C. (1998). Observations of substorm electrodynamics using MIRACLE network. In S. Kokobun & Y. Kamide (Eds.), *Substorms-4* (pp. 111–114). Tokyo: Terra Scientific Publishing Company.

Tanskanen, E. I. (2009). A comprehensive high-throughput analysis of substorms observed by IMAGE magnetometer network: Years 1993–2003 examined. *Journal of Geophysical Research*, *114*, A5. https://doi.org/10.1029/2008JA013682

Tanskanen, E. I., Pulkkinen, T. I., Viljanen, A., Mursula, K., Partamies, N., & Slavin, J. A. (2011). From space weather to space climate time scales: Substorm analysis from 1993 to 2008. *Journal of Geophysical Research*, *116*, A00I34. https://doi.org/10.1029/2010JA015788

Tanskanen, E. I., Slavin, J. A., Tanskanen, A., Viljanen, A., Pulkkinen, T. I., Koskinen, H. E. J., … Eastwood, J. (2005). Magnetospheric substorms are strongly modulated by interplanetary high-speed streams. *Geophysical Research Letters*, *32*, L16104. https://doi.org/10.1029/2005GL023318

Tokumaru, M., Kojima, M., Fujiki, K., & Hayashi, K. (2009). Non-dipolar solar wind structure observed in the cycle 23/24 minimum. *Geophysical Research Letters*, *36*, L09101. https://doi.org/10.1029/2009GL037461

Wang, Y.-M. (2016). Surface flux transport and the evolution of the Sun's polar fields. *Space Science Reviews*, *1-15*. https://doi.org/10.1007/s11214-016-0257-0

Zhao, H., & Zong, Q.-G. (2012). Seasonal and diurnal variation of geomagnetic activity: Russell-McPherron effect during different IMF polarity and/or extreme solar wind conditions. *Journal of Geophysical Research*, *117*, A11222. https://doi.org/10.1029/2012JA017845